



NIST  
PUBLICATIONS

**NIST** United States Department of Commerce  
Technology Administration  
National Institute of Standards and Technology

*NIST Technical Note 1502*

**Uncertainties in NIST Noise-  
Temperature Measurements**

J. Randa

QC  
100  
.U5753  
NO. 1502  
1998



*NIST Technical Note 1502*

# **Uncertainties in NIST Noise-Temperature Measurements**

J. Randa

Electromagnetic Fields Division  
Electronics and Electrical Engineering Laboratory  
National Institute of Standards and Technology  
325 Broadway  
Boulder, Colorado 80303-3328

March 1998



---

**U.S. DEPARTMENT OF COMMERCE**, William M. Daley, Secretary  
**TECHNOLOGY ADMINISTRATION**, Gary R. Bachula, Acting Under Secretary for Technology  
**NATIONAL INSTITUTE OF STANDARDS AND TECHNOLOGY**, Raymond G. Kammer, Director

National Institute of Standards and Technology Technical Note  
Natl. Inst. Stand. Technol., Tech. Note 1502, 52 pages (March 1998)  
CODEN:NTNOEF

U.S. GOVERNMENT PRINTING OFFICE  
WASHINGTON: 1998

---

For sale by the Superintendent of Documents, U.S. Government Printing Office, Washington, DC 20402-9325

## CONTENTS

	Page
1. INTRODUCTION.....	2
2. BACKGROUND AND NOTATION .....	3
3. WAVEGUIDE SYSTEMS WITH SIX-PORT REFLECTOMETERS .....	6
3.1 Cryogenic Standard .....	6
3.2 Ambient Standard .....	7
3.3 Power Ratios .....	7
3.4 Mismatch Factors .....	8
3.5 Asymmetry .....	11
3.6 Connector .....	12
3.7 Isolation .....	13
3.8 Frequency Offset (Broadband Mismatch) .....	14
3.9 Nonlinearity .....	16
3.10 Type-A Uncertainty .....	17
3.11 Combined Uncertainty .....	21
4. COAXIAL SYSTEMS WITH SIX-PORT REFLECTOMETERS .....	21
4.1 Cryogenic Standard .....	21
4.2 Ambient Standard .....	24
4.3 Power Ratios .....	24
4.4 Mismatch Factors .....	24
4.5 Asymmetry .....	26
4.6 Connector .....	26
4.7 Isolation.....	28
4.8 Frequency Offset (Broadband Mismatch) .....	28
4.9 Nonlinearity .....	29
4.10 Type-A and Combined Uncertainties .....	29
5. OTHER SYSTEMS .....	30
5.1 WR-90 (8 GHz to 12.4 GHz) Switching Radiometer .....	30
5.2 Tuned Systems for 30 and 60 MHz .....	32
6. MEASUREMENTS THROUGH ADAPTERS .....	33
6.1 Background .....	33
6.2 Uncertainty Analysis .....	38

7.	SUMMARY .....	41
8.	REFERENCES .....	42
	APPENDIX .....	44

# UNCERTAINTIES IN NIST NOISE-TEMPERATURE MEASUREMENTS

J. Randa  
Electromagnetic Fields Division  
National Institute of Standards and Technology  
325 Broadway  
Boulder, CO 80303

Uncertainty analyses are presented for NIST measurements of noise temperature. All systems currently used in NIST calibrations of thermal-noise sources are treated. These include tuned systems for 30 and 60 MHz, coaxial total-power radiometers for 1 to 12 GHz, a switching radiometer for the WR-90 (8.2 to 12.4 GHz) waveguide band, and total power waveguide radiometers for the WR-62 (12.4 to 18 GHz), WR-42 (18 to 26.5 GHz), WR-28 (26.5 to 40 GHz), and WR-15 (50 to 75 GHz) bands. Measurements through adapters are also analyzed. Typical expanded ( $k = 2$ ) uncertainties for the measurements are in the range 0.7 percent to 1.4 percent, depending on the particular system and the frequency.

Keywords: noise; noise measurement; noise temperature; thermal noise; uncertainty analysis

## 1. INTRODUCTION

The National Institute of Standards and Technology (NIST) offers noise-temperature measurement services covering a wide range of frequencies and connectors. A tuned coaxial radiometer is used for measurements at 30 MHz and 60 MHz [1]. For frequencies of 1 GHz and above, almost all the measurement systems are total-power radiometers, with internal six-port reflectometers to measure the relevant reflection coefficients [2-4]. The systems currently in use include coaxial radiometers covering 1 GHz to 12 GHz [2,3], as well as waveguide radiometers for the WR-62 (12.4 GHz to 18 GHz), WR-42 (18 GHz to 26.5 GHz), and WR-28 (26.5 GHz to 40 GHz) bands [2,4]. Coaxial sources are also measured from 12.4 GHz to 26.5 GHz using the waveguide radiometers and characterized adapters. One waveguide radiometer of a different basic design is a switching, or Dicke, radiometer [5,6] for the WR-90 (8 GHz to 12.4 GHz) waveguide band.

The many different systems and our understanding of them have evolved considerably over the years, with concomitant changes in the uncertainty analyses. Even for systems whose uncertainties have not changed, the method of reporting the uncertainties has changed. Prior to about 1993 the common practice in the NIST Noise Project was to compute and quote a worst-case or maximum possible error. This was done by estimating the maximum possible value for each component of the uncertainty and then forming the linear sum of the individual components. In 1992 NIST officially adopted the policy of reporting uncertainties which conform to the ISO guidelines [7,8]. Accordingly, the measurement services offered by the Noise Project now quote an expanded ( $2\sigma$ ) uncertainty, corresponding to a 95 percent confidence level. This required a conversion from worst-case errors to standard uncertainties for the individual components of uncertainty, as well as a change in the manner of combining the components. As a result of all these changes—in the systems, the analyses, and the method of reporting the uncertainty—the uncertainty analysis for a typical system is now scattered in several different places, often rather inaccessible, and there are sometimes conflicting forms for one analysis. The present paper addresses this problem; it assembles, reconciles, improves (in some cases), and presents the uncertainty analysis for each of the

systems currently used in noise-temperature measurements.

The next section establishes notation and provides some background. Section 3 contains the uncertainty analysis for the waveguide systems with total-power radiometers and built-in six-port reflectometers. It presents the estimates of the individual components of the uncertainty as well as the method of combining them. The similar coaxial systems for 1 GHz to 12 GHz are treated in Section 4. Section 5 deals with the WR-90 switching radiometer and the tuned coaxial system. The uncertainty analysis for measurements made through adapters is presented in Section 6. Section 7 contains a brief summary. There is one appendix, devoted to the philosophy and practice of converting from worst-case errors to standard uncertainties.

## 2. BACKGROUND AND NOTATION

In keeping with the notation of references [7] and [8], we will use  $u_{T_x}$  to denote the standard uncertainty in the measurement of  $T_x$ . The combined standard uncertainty is composed of type-A and type-B uncertainties. Type-A uncertainties are those that are measured and determined by statistical methods, typically the standard deviation of the mean of several independent measurements of the quantity of interest. Type-B uncertainties are those determined by other means, such as estimates of systematic uncertainties. We shall deal primarily with type-B uncertainties; the type-A uncertainty is treated near the end of each section. We use  $\mathcal{E}$  to denote the fractional standard uncertainty in a parameter, for example,  $\mathcal{E}_{C_{ry}} = u_{T_{Cry}}/T_{Cry}$ . Because we must deal with uncertainty estimates which predate the ISO definition of standard uncertainty, we need notation for other types of uncertainty estimates. For nonstandard uncertainties, such as worst-case errors, we use the symbol  $\Delta$  with the relevant variable or parameter. Thus  $\Delta T_{amb}$  would be the worst-case error in the ambient temperature. The relation between worst-case error and standard uncertainty is discussed in detail in the Appendix. The symbol  $\delta$  will be used to denote arbitrary (small) variations in a parameter. This is used in calculations of the propagation of uncertainties, to determine how the uncertainty in the quantity of interest is related to the uncertainties in the various other

measured (or estimated) quantities. These variations in a parameter ( $z$ , for example) can be related to the standard uncertainty in the parameter by

$$u_z^2 = \langle |\delta z|^2 \rangle, \quad (1)$$

where the average is taken over the typical variations occurring in that parameter in a (very large) set of independent measurements.

For the NIST total-power radiometers, which are dealt with in Sections 3 and 4, the equation used to compute the noise temperature of the device under test (DUT) is

$$T_x = T_a + \frac{M_s \eta_s (Y_x - 1)}{M_x \eta_x (Y_s - 1)} (T_s - T_a), \quad (2)$$

where a perfect isolator and a linear radiometer are assumed [2,4]. Equation (2) is referred to as the radiometer equation. The  $Y$ 's are the ratios of the detected power from the cryogenic standard or the DUT to the detected power from the ambient standard,  $Y_s = p_s/p_a$  and  $Y_x = p_x/p_a$ . To define the relevant reference planes for the mismatch factors ( $M$ ) and efficiencies ( $\eta$ ), we refer to fig. 1. The cryogenic standard, the ambient standard, and the DUT are connected to three different ports of the front-end switch of the radiometer. The mismatch factors in eq (2) are the ratios of delivered to available power at plane 3 for the cryogenic standard ( $M_s$ ) and at plane 2 for the DUT ( $M_x$ ). The efficiencies are ratios of delivered powers at two different planes. For the cryogenic standard,  $\eta_s = p_o(S)/p_3$ , and for the DUT,

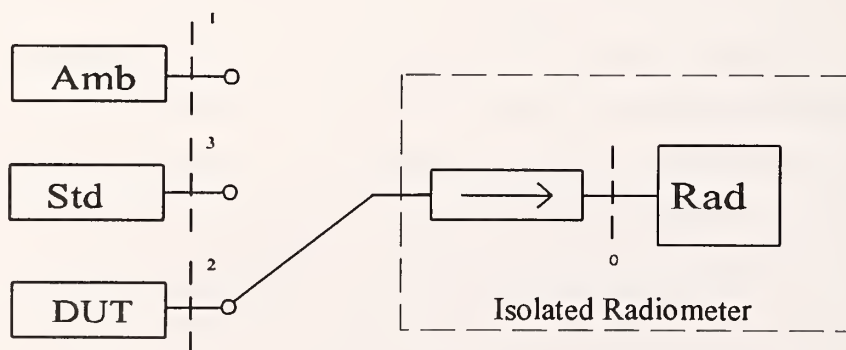


Figure 1. Basic setup for measurement of noise temperature.

$\eta_x = p_o(x)/p_2$ . The temperatures appearing in eq (2) are *noise* temperatures, which are related to the available noise power by  $P = k_B BT$ , where  $k_B$  is Boltzmann's constant, and  $B$  is the bandwidth. For a passive load, the noise temperature and the physical temperature  $T_{phys}$  are related by

$$k_B T_{noise} = \frac{hf}{e^{\left(\frac{hf}{k_B T_{phys}}\right)} - 1}, \quad (3)$$

where  $h$  is Planck's constant and  $f$  is the frequency. For low frequency or high temperature, the two are approximately equal.

Uncertainties in  $T_x$  arise due to uncertainties in the determination of the quantities appearing on the right side of eq (2) and due to departures from perfect isolation and linearity. For quantities appearing in eq (2), the propagation of uncertainties is treated in the usual manner. Thus, for example, the variation in  $T_x$  induced by a small variation in the cryogenic-standard temperature  $T_S$  is given by

$$\begin{aligned} \delta T_x(Cry) &= \frac{\partial T_x}{\partial T_S} = \frac{M_S \eta_S (Y_x - 1)}{M_x \eta_x (Y_S - 1)} \delta T_S \\ &= \left(1 - \frac{T_a}{T_x}\right) \frac{T_x}{T_S - T_a} \delta T_S, \end{aligned} \quad (4)$$

and thus

$$\frac{u_{T_x}(Cry)}{T_x} = \left|1 - \frac{T_a}{T_x}\right| \left|\frac{T_S}{T_a - T_S}\right| \frac{u_{Cry}}{T_S}. \quad (5)$$

The next two sections evaluate the individual components of the uncertainty for the waveguide and coaxial total-power radiometers used at 1 GHz and above. The bulk of each section is devoted to the type-B uncertainties arising in a single measurement of the unknown

noise temperature  $T_x$ . The type-A uncertainties evaluated from multiple measurements of  $T_x$  are treated near the end of each section. The tuned coaxial system for 30 MHz and 60 MHz and the WR-90 switching radiometer have different radiometer equations instead of eq (2) [1,6]. The uncertainties for these two systems are treated in Section 5.

### 3. WAVEGUIDE SYSTEMS WITH SIX-PORT REFLECTOMETERS

#### 3.1 Cryogenic Standard

The uncertainty in the noise temperature of the cryogenic standard contributes to the uncertainty in  $T_x$  as

$$\frac{u_{T_x}(Cry)}{T_x} = \left| 1 - \frac{T_a}{T_x} \right| \left| \frac{T_s}{T_a - T_s} \right| \mathcal{E}_{Cry}. \quad (6)$$

The fractional uncertainty in the noise temperature of the cryogenic standard,  $\mathcal{E}_{Cry}$ , depends on which specific standard is used. There is a different cryogenic primary standard for each waveguide band.

The design and the analysis of the worst-case error for the WR-10 waveguide primary standard are contained in reference [9]. The same basic uncertainty analysis applies to the cryogenic standards in the other waveguide bands, with different numerical values for the individual components of the uncertainty. A notebook kept in the calibration laboratory and entitled "Thermal Noise Standards: Calculations and User's Manual" contains calculations of the worst-case uncertainty for each of the NIST waveguide noise standards. It lists the different components of the uncertainty for each standard, giving a worst-case value for each. These values reflect an improved understanding of the uncertainties in the resistivity of the gold-plated horns, but otherwise are based on the analysis of reference [9]. As discussed in the Appendix, we convert each worst-case value to a standard uncertainty by dividing by  $\sqrt{3}$ . The three principal components are the neglected excess radiation from the cavity walls, the

uncertainty in the load temperature, and the uncertainty in the noise efficiency. These three are not correlated, and so we are justified in combining them incoherently using root sum of squares (RSS). When we do so, the values obtained for the primary standards in the different waveguide bands are

$$\mathcal{E}_{CRY} = \begin{array}{ll} 0.18\% & WR-90 \\ 0.22\% & WR-62 \\ 0.26\% & WR-42 \\ 0.17\% & WR-28 \\ 0.39\% & WR-22 \\ 0.48\% & WR-15. \end{array} \quad (7)$$

We shall use the values of eq (7) in eq (6) for the contribution of the cryogenic standard uncertainty to the standard uncertainty in  $T_x$ .

### 3.2 Ambient Standard

The contribution of the uncertainty in the ambient standard temperature to the uncertainty in the DUT noise temperature is given by

$$\frac{u_{T_x}(amb)}{T_x} = \left| \frac{T_x - T_s}{T_a - T_s} \right| \frac{T_a}{T_x} \mathcal{E}_{T_a}. \quad (8)$$

The ambient standard consists of a waveguide termination held at a constant temperature by a water jacket with circulating room-temperature water. The water jacket is itself enveloped in an insulating blanket. The physical temperature of the termination is measured with a calibrated thermistor. A conservative estimate of the uncertainty in the temperature measurement is  $u_{T_a} = 0.1$  K, and thus  $\mathcal{E}_{T_a} = 0.034$  percent.

### 3.3 Power Ratios

The measured powers enter the radiometer equation through the ratios  $Y_x \equiv p_x/p_a$  and  $Y_s \equiv p_s/p_a$  in the factor  $(Y_x - 1)/(Y_s - 1)$ , which we define as  $Y$ . An analysis of the uncertainty

in  $Y$  is outlined by S. Pucic in reference [10]. She parameterizes the effective efficiency of the thermistor mount as  $\eta_e = \eta_{e0} + kp$  and then derives the expression for the uncertainty in  $Y$  due to the uncertainty in  $k$ . Her expression can be simplified and put into the form

$$u_Y = \eta_{e0} \left| \frac{Y_x - 1}{1 - Y_s} \right| \frac{|p_x - p_s|}{(\eta_{e0} - kp_a)^2} u_k. \quad (9)$$

The resulting uncertainty in the DUT noise temperature is

$$\begin{aligned} \frac{u_{T_x}(Y)}{T_x} &= \left| \frac{T_s - T_a}{T_x} \right| u_Y \\ &= \frac{\eta_{e0}}{(\eta_{e0} - kp_a)^2} \left| 1 - \frac{T_a}{T_x} \right| |p_x - p_s| u_k. \end{aligned} \quad (10)$$

Personnel of the NIST Microwave Power Project indicate that the best that they can do in measuring linearity with a NIST Type-IV power meter is  $\pm 0.1$  percent over a range of 10 mW. We assume that we can do half as well and take  $u_k = 0.02$  percent per milliwatt. Since  $\eta_{e0} \approx 1$  and  $kp_a \ll 1$ , and since we keep  $p_x$  and  $p_s$  less than about 2 mW in our measurements, eq (10) then implies that

$$\frac{u_{T_x}(Y)}{T_x} \leq \left| 1 - \frac{T_a}{T_x} \right| \times 0.04\%, \quad (11)$$

which is negligible unless  $T_a \geq 3 T_x$ .

### 3.4 Mismatch Factors

The mismatch ratio is one of the principal sources of uncertainty. It contributes to the uncertainty in the DUT noise temperature according to

$$\frac{u_{T_x}(M/M)}{T_x} = \left| 1 - \frac{T_a}{T_x} \right| \mathcal{E}_{M/M}. \quad (12)$$

Because the ratio of mismatch factors is very near 1,  $\mathcal{E}_{M/M} = u_{M/M}/(M/M) \approx u_{M/M}$ . The mismatch-factor ratio itself is given by

$$\frac{M_S}{M_x} = \frac{(1 - |\Gamma_S|^2)(1 - |\Gamma_{r,S}|^2)}{|1 - \Gamma_S \Gamma_{r,S}|^2} \frac{|1 - \Gamma_x \Gamma_{r,x}|^2}{(1 - |\Gamma_x|^2)(1 - |\Gamma_{r,x}|^2)}, \quad (13)$$

where the subscript  $S$  denotes the cryogenic standard, the subscript  $r,S$  denotes the radiometer as seen from the standard's port, etc. If we compute the variation in  $M_S/M_x$  due to small variations in the  $\Gamma$ 's, we get

$$\delta \left( \frac{M_S}{M_x} \right) \approx -2(x_S - x_{r,S})(\delta x_S - \delta x_{r,S}) - 2(y_S + y_{r,S})(\delta y_S + \delta y_{r,S}) \\ + 2(x_x - x_{r,x})(\delta x_x - \delta x_{r,x}) + 2(y_x + y_{r,x})(\delta y_x + \delta y_{r,x}), \quad (14)$$

where  $x$  and  $y$  refer to real and imaginary parts of  $\Gamma$ , and where we have assumed that the reflection coefficients are small. To obtain  $u_{M/M}$  from eq (14) we need to know whether the various  $\delta x$ 's and  $\delta y$ 's are correlated. If they are all perfectly correlated (i.e., if all the  $\delta x$ 's and  $\delta y$ 's are equal), then

$$u_{M/M}(cor.) = 4 u_{Im\Gamma} |y_S + y_{r,S} - y_x - y_{r,x}|. \quad (15)$$

This is the corrected version of the form in reference [2]. If the  $\delta x$ 's and  $\delta y$ 's are all entirely uncorrelated, eq (14) leads to

$$u_{M/M}(uncor.) = 2\sqrt{2} u_{Re\Gamma} [(x_S - x_{r,S})^2 + (y_S + y_{r,S})^2 \\ + (x_x - x_{r,x})^2 + (y_x + y_{r,x})^2]^{\frac{1}{2}}, \quad (16)$$

where we have assumed  $u_{Re\Gamma} = u_{Im\Gamma}$ . Consultation with the NIST Network Analysis and Measurements Project indicates that we should expect the variations to be correlated (for small  $|\Gamma|$ ), which means that eq (15) would be appropriate. We are uncomfortable with eq (15), however, particularly when the imaginary parts in eq (15) nearly cancel and we have to

rely on the equality of the variations in eq (14) to eliminate any effect of the real parts. This is particularly unsettling since the mismatch factors are a major source of uncertainty. To be safe, we shall use the maximum of eqs (15) and (16), thereby protecting ourselves from artificially small uncertainties due to chance cancellations.

The remaining question is what is  $u_{Re\Gamma}$ ? The values for  $u_{Re\Gamma}$  measured with our commercial vector network analyzer (VNA) are about 0.0013 for WR-62 and WR-42, and about 0.001 for WR-28 with a precision calibration. In the checkout of each of the noise-temperature measurement system, we compared the results for reflection coefficients measured with the system six-port to those measured with the VNA or by the NIST Network Analysis and Measurements Project. The agreement required varied from system to system. For WR-62 each reflection coefficient was measured many times on the system six-port, and we required that the system six-port results agreed with the VNA results to within a standard deviation of the six-port results. For WR-42 we required that the average of the six-port measurements agreed with the VNA results within 0.007. For WR-28 we required agreement within 0.014. For WR-28 we also did additional comparisons to the VNA and to the Network Analysis and Measurements Project. Those agreed to within 0.002 for  $|\Gamma|$  and about 0.007 or 0.008 for  $\text{Im } \Gamma$ . In the initial certification of the WR-15 system, the agreement was within 0.004, but the check was performed only at 63 GHz. Since the levels of agreement were never exceeded in the tests, we take them to be expanded uncertainties, and we divide them by 2 to obtain the standard uncertainties. We then have

$$u_{Re\Gamma} = \begin{array}{ll} 0.0035 & WR-62, WR-42 \\ 0.007 & WR-28, WR-15. \end{array} \quad (17)$$

The WR-15 uncertainty was increased to the value of the WR-28 uncertainty because of the lack of information across the entire band.

To summarize, in eq (12) we use  $\mathcal{E}_{MM} \approx u_{MM}$  and

$$u_{M|M} = \text{Max} \{u_{M|M}(\text{cor.}), u_{M|M}(\text{uncor.})\}, \quad (18)$$

with  $u_{MM}(\text{cor.})$  and  $u_{MM}(\text{uncor.})$  given by eqs (15) and (16), and with  $u_{\text{Re}\Gamma}$  given by eq (17).

### 3.5 Asymmetry

The asymmetry is defined as the ratio of efficiencies  $\eta_s/\eta_x$  appearing in the radiometer equation. Its contribution to the uncertainty in the measured noise temperature is

$$\frac{u_{T_x}(\eta/\eta)}{T_x} = \left| 1 - \frac{T_a}{T_x} \right| u_{\eta/\eta}, \quad (19)$$

where we have used  $\mathcal{E}_{\eta/\eta} \approx u_{\eta/\eta}$ . Reference [2] derived a value of 0.23 percent for the worst-case error in the asymmetry. That was based on an analysis of the uncertainty in the measurements of the power ratios which occur in the asymmetry measurement. However, the basis for that analysis has been superseded by subsequent work [10], which found that the power-ratio uncertainty is negligible. Consequently, we must reexamine the uncertainty in the asymmetry.

The method for measuring the asymmetry is detailed in references [2] and [4]. Two noise sources ( $x1$  and  $x2$ ) are attached to the two ports ( $x1$  on the standard port and  $x2$  on the DUT port), and we measure the delivered power and mismatch factor of each. The two sources are interchanged and the measurement is repeated. If we use primed quantities to denote the second (interchanged) configuration, the expression for the asymmetry in terms of measured quantities is [2,4]

$$\frac{\eta_s}{\eta_x} = \sqrt{\frac{M_{x1} M'_{x2} (Y_{x2} - 1) (Y'_{x1} - 1)}{M_{x2} M'_{x1} (Y'_{x2} - 1) (Y_{x1} - 1)}}, \quad (20)$$

Where the  $Y$  factors are the ratios of the delivered power from the designated source to the delivered power from the ambient standard,  $Y_{x1}' = p_{x1}'/p_a$ , etc. The uncertainty in this

determination of the asymmetry is dominated by the uncertainty in the measurement of the ratios of mismatch factors,

$$\delta_{\eta/\eta} \approx \delta_{M/M} + \delta_{M'/M'} \quad (21)$$

In principle, we could use the relevant  $\Gamma$ 's to evaluate the mismatch-ratio uncertainties using eq (15) or (16), but the system software does not allow this. Instead we will use a conservative estimate of the typical size of  $u_{M/M}$ . This is obtained by squaring and averaging the expression in eq (14), and assuming the average of each reflection coefficient is 0.1. That leads to

$$\begin{aligned} \langle u_{M/M}^2 \rangle &= 8 \langle x_S^2 + x_{r,S}^2 + y_S^2 + y_{r,S}^2 + x_x^2 + x_{r,x}^2 \\ &\quad + y_x^2 + y_{r,x}^2 \rangle u_{Re\Gamma}^2, \end{aligned} \quad (22)$$

$$u_{\eta/\eta} \approx 0.4 u_{Re\Gamma}. \quad (23)$$

With the values of  $u_{Re\Gamma}$  from the preceding section (0.0035 for WR-62 and WR-42, 0.007 for WR-28 and WR-15), we then have

$$\begin{aligned} u_{\eta/\eta} &= 0.28\% \quad WR-62, WR-42 \\ &0.56\% \quad WR-28, WR-15. \end{aligned} \quad (24)$$

These values are used in eq (19) to compute the asymmetry contribution to the uncertainty in the DUT noise temperature. The values of eq (24) are quite large, particularly for WR-28 and WR-15, and are not on a very firm footing. They are safe, but it may be possible to reduce them significantly with some additional work.

### 3.6 Connector

Additional uncertainty arises from the variability from one waveguide flange to another, even when both meet specifications. Such variations are already included in our estimates of  $u_{Re\Gamma}$ , and they require no further special treatment for their effects on mismatch

factors. They do, however, affect the measurement of the asymmetry, and this effect was not included in  $u_{T_x}(\eta/\eta)$ . When the asymmetry is measured, noise sources are attached to the ports of interest, and the delivered powers are measured. When this asymmetry is used in a calibration, we assume that the connectors of the DUT and the primary standard are identical. The error in that assumption can be written as

$$\frac{\Delta T_x}{T_x} = \left| 1 - \frac{T_a}{T_x} \left| \frac{\eta_{sc}}{\eta_{xc}} - 1 \right| \right|, \quad (25)$$

where the last term contains the ratio of the efficiencies of the cryogenic-standard connector and the DUT connector. This last term was estimated in reference [2]. Subsequent revisions resulted in a value of  $\pm 0.003 \text{ dB} \times f^{1/2}(\text{GHz})$  for the range of the term  $|\eta/\eta-1|$ , which we will use as the standard uncertainty in that quantity. To convert from decibels to a natural number we multiply by 0.23, thereby obtaining

$$\frac{u_{T_x}(\text{conn})}{T_x} = 0.069\% \left| 1 - \frac{T_a}{T_x} \right| \sqrt{f}, \quad (26)$$

where  $f$  is in gigahertz. This is a sizable contribution to the uncertainty, roughly 0.4 percent for a typical device at 36 GHz, and is probably an overestimate. An improved analysis could reduce this uncertainty significantly.

### 3.7 Isolation

Reference [2] derived an equation for the worst-case error in  $T_x$  due to imperfect isolation,

$$\frac{\Delta T_x(\text{isol})}{T_x} = 0.01 \times \left\{ 0.47 |\Gamma_S| \left| 1 - \frac{T_a}{T_x} \right| + 0.047 \left| 1 - \frac{T_S}{T_x} \right| + 100 \frac{|\Gamma_x|}{T_x} \right\}, \quad (27)$$

where  $T_x$  is in kelvins. This form assumes isolation of at least 50 dB. The WR-62, WR-42,

and WR-28 systems all have been measured to have greater than 50 dB isolation across their entire bands. There was a minor arithmetic error in deriving eq (27) [2]; 0.47, 0.047, and 100 should be changed to 0.48, 0.048, and 108, respectively. Equation (27) represents a worst-case uncertainty. In this case, we are very confident ( $\geq 95$  percent) that the true error is less than that given by eq (27), and so we divide by 2 (and assume a normal distribution) to get the standard uncertainty,

$$\frac{u_{T_x}(isol)}{T_x} = 0.01 \times \left\{ 0.24 |\Gamma_S| \left| 1 - \frac{T_a}{T_x} \right| + 0.024 \left| 1 - \frac{T_S}{T_x} \right| + 54 \frac{|\Gamma_x|}{T_x} \right\} \quad (28)$$

for WR-62, WR-42, and WR-28. This is generally less than 0.03 percent. For WR-15 the isolation was measured to be greater than 45 dB across the band. In that case,

$$\frac{u_{T_x}(isol)}{T_x} = 0.01 \times \left\{ 0.45 |\Gamma_S| \left| 1 - \frac{T_a}{T_x} \right| + 0.045 \left| 1 - \frac{T_S}{T_x} \right| + 101 \frac{|\Gamma_x|}{T_x} \right\}, \quad (29)$$

which is typically about 0.05 percent.

### 3.8 Frequency Offset (Broadband Mismatch)

This uncertainty arises from the fact that the reflection coefficients, and hence the mismatch factors, are measured at the nominal measurement frequency, with negligible bandwidth, whereas the power measurements are made across a bandwidth as large as tens of megahertz, the center of which is offset from the nominal measurement frequency by the intermediate frequency (IF). The uncertainty introduced by possible variation of the mismatch factors across the measurement band is called the broadband mismatch uncertainty. The uncertainty due to the center of the measurement band being at  $f \pm f_{IF}$  rather than at  $f$  is called the frequency-offset uncertainty. Typical commercial noise sources have reflection coefficients which are essentially constant for such frequency differences. The same is not true for the radiometer itself, however. There is a significant length of transmission line

between the input ports (planes 2 and 3) and the isolator, which is the principal source of reflections from the radiometer. Consequently, as the frequency changes, the phase of the reflected wave observed at plane 2 or 3 will vary, even if the reflection from the isolator is constant. The worst-case uncertainty due to this effect was calculated in reference [2]. (Slightly different forms were derived in references [11] and [12], but we shall use the more conservative form of reference [2].) To convert from worst-case to standard uncertainty we assume a uniform distribution and divide the result of reference [2] by  $\sqrt{3}$ . This yields

$$\frac{u_{T_x}(BBMM)}{T_x} = \frac{200\%}{\sqrt{3}} \left| \cos\left(\frac{4\pi f_{IF} l_e}{30}\right) \text{sinc}\left(\frac{\pi B l_e}{15}\right) - 1 \right| \quad (30)$$

$$\times (|\Gamma_S \Gamma_{r,S}| + |\Gamma_x \Gamma_{r,x}|) \left| 1 - \frac{T_a}{T_x} \right|,$$

where  $f_{IF}$  is the intermediate frequency,  $B$  is the IF bandwidth, and  $\text{sinc } x \equiv (\sin x)/x$ . The electrical length  $l_e$  is related to the distance  $l$  from input port to isolator by

$$l_e = l \sqrt{1 - \frac{f_c^2}{f^2}}, \quad (31)$$

where  $f_c$  is the cutoff frequency of the waveguide. The values of the parameters for the different NIST waveguide systems are given in Table 1. Although  $f_{IF}$  is nominally 0, there is

Table 1: System parameters for use in eqs (30) and (31).

System	$f_{IF}$ (GHz)	$B$ (GHz)	$f_c$ (GHz)	$l$ (cm)
WR-62	0	0.040	9.49	56.
WR-42	0	0.040	14.1	43.5
WR-28	0	0.040	21.1	50.
WR-15	0	0.040	39.9	36.

in fact a narrow notch in the frequency response at 0, due to the low-frequency response of the mixer used in the down conversion. The shape of the frequency-response curve is accounted for in the noise-temperature measurements. Its effect on the uncertainty estimate is negligible, and we can use eq (30), which was derived with the assumption of a flat response across the IF bandwidth.

### 3.9 Nonlinearity

The final contribution to the type-B uncertainty is due to the possibility of small nonlinear behavior by the radiometer. Reference [2] derives an expression for this uncertainty, but this result was subsequently subjected to major revisions. Rather than try to resurrect the old analysis, we use our routine IF linearity checks [4] to place a limit on the uncertainty due to nonlinear behavior.

Our routine linearity test consists of switching a (nominally) 3-dB pad in and out of the measurement circuit, in front of the IF amplifier. The ratio of the two output powers is measured and plotted as a function of input power. The "linear" result is established by averaging the low-power points, and we then require that the ratio not deviate from the linear result by more than 0.005 dB (0.12 percent). The nonlinearity in the IF amplifier can be parameterized by [2]

$$\begin{aligned}
 P_{out} &= \frac{g_2}{1 + \frac{a g_2}{k} P_{in}} P_{in} \\
 &\approx g_2 P_{in} (1 - \alpha P_{in}),
 \end{aligned}
 \tag{32}$$

where  $\alpha = a g_2 / k$ . The ratio of output powers for the case of  $p_{2,in} = 2 p_{1,in}$  is then given by

$$\begin{aligned} \frac{P_{2,out}}{P_{1,out}} &\approx \frac{P_{2,in}}{P_{1,in}} [1 - \alpha (P_{2,in} - P_{1,in})] \\ &= 2 (1 - \alpha P_{1,in}). \end{aligned} \quad (33)$$

The linearity check assures us that  $\alpha P_{1,in} \leq 0.12$  percent. That is a worst-case error; we'll take the standard uncertainty to be half that, 0.06 percent. This introduces a corresponding 0.06 percent uncertainty into the measurement of  $Y_x$  since the nonlinearity is negligible for measurement of  $P_a$ . The resulting uncertainty in  $T_x$  is given by

$$\begin{aligned} \frac{u_{T_x}(lin)}{T_x} &= \left| 1 - \frac{T_a}{T_x} \right| \frac{u_{y_x}}{|Y_x - 1|} \\ &= \frac{u_{y_x}}{Y_x} = 0.06\%. \end{aligned} \quad (34)$$

### 3.10 Type-A Uncertainty

In noise-temperature calibrations using our waveguide total-power radiometers, we repeat measurements on several different levels. Typically we do three independent calibrations of the entire system (six-port calibration plus asymmetry measurement). For each of these three calibrations we perform one (for "mature" systems) or more (three for WR-28) separate measurements of the reflection coefficients of the cryogenic standard and the DUT. And for each of these separate measurements we do a number of readings (typically 20) of the delivered powers from the two standards and from the DUT. A noise temperature of the DUT is computed for each DUT power reading. Thus, in a typical WR-28 calibration, we have three system calibrations times three measurements times twenty readings, for a total of 180 values of the noise temperature, which are combined to obtain the final value for the measured DUT noise temperature. The question is how to evaluate the type-A uncertainty in obtaining the average value from the multiple measurements.

We use  $T_{ijk}$  for the value of a single reading of the noise temperature. The index  $i$ , which denotes the number of the system calibration, runs from 1 to  $N_C$ ; the index  $j$  denotes the measurement number and runs from 1 to  $N_M$ ; the index  $k$  denotes the reading number and runs from 1 to  $N_R$ . We assume that the number of readings  $N_R$  is the same for each measurement and that the number of measurements  $N_M$  is the same for each calibration. We use  $T_{ij}$  to denote the mean of the  $N_R$  readings for each measurement and use  $\sigma_{ij}$  for the associated standard deviation,

$$T_{ij} = \frac{1}{N_R} \sum_{k=1}^{N_R} T_{ijk},$$

$$\sigma_{ij}^2 = \frac{1}{(N_R - 1)} \sum_{k=1}^{N_R} (T_{ij} - T_{ijk})^2.$$
(35)

Similarly, we use  $T_i$  and  $\sigma_i$  for the mean and standard deviation of the  $N_M$  measurements for calibration  $i$ ,

$$T_i = \frac{1}{N_M} \sum_{j=1}^{N_M} T_{ij},$$

$$\sigma_i^2 = \frac{1}{(N_M - 1)} \sum_{j=1}^{N_M} (T_i - T_{ij})^2,$$
(36)

and we use  $T$  and  $\sigma$  for the mean and standard deviation of the  $N_C$  calibrations,

$$T = \frac{1}{N_C} \sum_{i=1}^{N_C} T_i,$$

$$\sigma^2 = \frac{1}{(N_C - 1)} \sum_{i=1}^{N_C} (T - T_i)^2.$$
(37)

Reference [4] reported that we use the standard deviation of the mean of the  $N_C$  values of  $T_i$  as the type-A uncertainty. It was recognized in reference [4] that this was not entirely

correct, but it was very close for the WR-62 and WR-42 systems and for some frequencies for WR-28. In some recent cases in WR-28, however, it became clear that this estimate is inadequate, and we must modify our computation of  $u_A$ . In particular, the spread in the 20 readings for a single measurement is far from negligible and is not accounted for in the previous evaluation.

To develop the more general expression for  $u_A$  we model [13] the variable  $T_{ijk}$  as

$$T_{ijk} = \tau + C_i + M_{ij} + R_{ijk}, \quad (38)$$

where  $\tau$  is the true value for the noise temperature of the device being measured,  $C_i$  is a random variable representing variations from calibration to calibration,  $M_{ij}$  is a random variable representing variations from measurement to measurement ( $j$ ), which also varies from calibration to calibration ( $i$ ), and  $R_{ijk}$  is a random variable which varies with the reading  $k$ , the measurement  $j$ , and the calibration  $i$ . Our estimate of the true value is just the mean of all the readings,

$$\tau \approx T \equiv \frac{1}{N_C N_M N_R} \sum_{i=1}^{N_C} \sum_{j=1}^{N_M} \sum_{k=1}^{N_R} T_{ijk}. \quad (39)$$

The means of the three random variables are all 0, and their variances will be denoted by

$$\begin{aligned} \langle C_i^2 \rangle &= v_C, \\ \langle M_{ij}^2 \rangle &= v_M, \\ \langle R_{ijk}^2 \rangle &= v_R, \end{aligned} \quad (40)$$

where the averages are over all indices. The variances can be estimated from the measured values  $T_{ijk}$  by

$$\begin{aligned}
\frac{1}{N_C N_M (N_R - 1)} \sum_{ijk} (T_{ijk} - T_{ij})^2 &\approx v_R, \\
\frac{1}{N_C (N_M - 1)} \sum_{ij} (T_{ij} - T_i)^2 &\approx v_M + \frac{v_R}{N_R}, \\
\frac{1}{(N_C - 1)} \sum_i (T_i - T)^2 &\approx v_C + \frac{v_M}{N_C} + \frac{v_R}{N_C N_R}.
\end{aligned} \tag{41}$$

The equalities are only approximate because we are dealing with a limited sample. We can solve eq (41) for  $v_R$ ,  $v_M$ , and  $v_C$ , and use eqs (35) through (37) to write

$$\begin{aligned}
v_R &= \langle \sigma_{ij}^2 \rangle, \\
v_M &= \langle \sigma_i^2 \rangle - \frac{v_R}{N_R}, \\
v_C &= \sigma^2 - \frac{v_M}{N_M} - \frac{v_R}{N_M N_R},
\end{aligned} \tag{42}$$

where the averages are over all free indices and where it is understood that if a negative value results for  $v_M$  or  $v_C$  it is taken to be 0. The type-A uncertainty in the determination of  $\tau \approx T$  is then the square root of the variance in  $T$ ,

$$u_A \approx \sqrt{\frac{v_C}{N_C} + \frac{v_M}{N_C N_M} + \frac{v_R}{N_C N_M N_R}}. \tag{43}$$

Comparison to the last line of eq (42) reveals that eq (43) is equivalent to  $u_A^2 = \sigma^2/N_C$ , provided that eq (42) does not result in a negative value for  $v_C$ . This is as it should be: if we did enough independent system calibrations to determine  $\sigma^2$  well, that would be sufficient, since it includes the variations from one reading to another and from one measurement to another. Since we only do three independent system calibrations, we supplement that information with the measured  $\sigma_i^2$  and  $\sigma_{ij}^2$ . Equation (43) is now used to evaluate the type-A uncertainties in the noise-temperature calibrations using our waveguide total-power radiometers.

### 3.11 Combined Uncertainty

The type-B standard uncertainty for a single noise temperature measurement is obtained by forming the square root of the sum of the squares of the individual contributions eqs (6, 8, 11, 18, 19, 26, 28 or 29, 30, 34),

$$u_B = [u_{T_x}^2(Cry) + u_{T_x}^2(amb) + u_{T_x}^2(Y) + u_{T_x}^2(M/M) + u_{T_x}^2(\eta/\eta) + u_{T_x}^2(con) + u_{T_x}^2(isol) + u_{T_x}^2(BBMM) + u_{T_x}^2(lin)]^{1/2}. \quad (44)$$

In calibrating a customer's device, we make several measurements of its noise temperature. Because the uncertainty defined by eq (44) depends on the measured noise temperature and on various measured reflection coefficients, it is in principle different for each of the separate measurements of the device's noise temperature. In practice, however, there is little difference between the values, and we use the maximum.

The expanded ( $k = 2$ ) combined uncertainty is computed from eqs (43) and (44),

$$U = 2\sqrt{u_A^2 + u_B^2}. \quad (45)$$

The expanded uncertainty varies with the device being tested, the frequency, and the waveguide band. At present, typical values of the expanded uncertainty for a source with high noise temperature (above a few thousand kelvins) are about 0.7 percent to 0.9 percent for the WR-62 and WR-42 systems, and 1.0 percent to 1.4 percent for WR-28. The WR-15 system is currently undergoing tests. When it is back in service, we expect its expanded uncertainties to be around 1.5 percent.

## 4. COAXIAL SYSTEMS WITH SIX-PORT REFLECTOMETERS

### 4.1 Cryogenic Standard

As was the case for the waveguide systems, the uncertainty in the noise temperature of the cryogenic standard contributes to the uncertainty in  $T_x$  as

$$\frac{u_{T_x}(\text{Cry})}{T_x} = \left| 1 - \frac{T_a}{T_x} \right| \left| \frac{T_s}{T_a - T_s} \right| \mathcal{E}_{\text{Cry}}. \quad (46)$$

At present there are two coaxial, cryogenic, primary standards used in noise-temperature measurements, called Standards C and D. A new standard, Standard E [14], is currently under test. Standards C and E have GPC-7 connectors, whereas Standard D has a precision type-N connector. Standards C and D are of nearly identical design, differing only in the output connector. Their uncertainties were originally analyzed in reference [15]. The analysis was later revised in an internal memorandum. The more recent result for the worst-case uncertainty is

$$\frac{\Delta T_{\text{Cry}}}{T_{\text{Cry}}} = [1.54 + (0.134 + 4.72 C_{03})f^{1/2} + 0.4A(f)]\%, \quad (47)$$

$$A(f) = (C_{01} + C_{02} + C_2)f^{1/2} + \frac{a_{11}}{1 + \frac{a_{12}}{f^2}},$$

where the frequency  $f$  is in gigahertz. The values of the parameters for the two standards can be found in Table 2. To compute a "standard" uncertainty from this worst-case value, we treat the separate contributions as independent and divide the root-sum-of-squares result by  $\sqrt{3}$ . That results in

$$\mathcal{E}_{\text{Cry}} = [1.813 + (0.01013 + 21.174 C_{03}^2)f + 0.16A(f)^2]^{1/2}/\sqrt{3}. \quad (48)$$

Numerical evaluation of eq (48) yields the fractional uncertainties of Table 3 for the two primary noise standards currently used in our coaxial calibrations. Equation (48) or Table 3 is then used in eq (46) to yield  $u_{T_x}(\text{Cry})$ .

Table 2. Parameters for evaluation of uncertainties in coaxial primary standards, eq (47).

	$C_{01}$	$C_{02}$	$C_2$	$C_{03}$	$a_{11}$	$a_{12}$
Std. C	0.0103	0.0060	0.0120	0.0245	0.0660	0.3654
Std. D	0.0092	0.0100	0.0080	0.0224	0.0450	0.3020

Table 3. Standard fractional uncertainty in noise temperatures of coaxial primary standards.

f(GHz)	$\mathcal{E}(\text{Std. C}), \%$	$\mathcal{E}(\text{Std. D}), \%$
1.0	0.782	0.782
2.0	0.787	0.786
3.0	0.792	0.791
4.0	0.797	0.795
5.0	0.802	0.800
6.0	0.807	0.804
7.0	0.812	0.808
8.0	0.816	0.813
9.0	0.821	0.817
10.0	0.826	0.821
11.0	0.830	0.825
12.0	0.835	0.830

## 4.2 Ambient Standard

The contribution of the uncertainty in the ambient standard temperature to the uncertainty in the DUT noise temperature is given by

$$\frac{u_{T_x}(amb)}{T_x} = \left| \frac{T_x - T_s}{T_a - T_s} \right| \frac{T_a}{T_x} \mathcal{E}_{T_a}. \quad (49)$$

The temperature of the ambient standard for the coaxial system is measured with a glass-mercury thermometer rather than a thermistor as in the waveguide case. Comparison of the thermometer to a thermistor calibrated by NIST ( $\pm 0.002$  K) indicated agreement to within  $\pm 0.02$  K. The other contribution to the uncertainty in the temperature of the ambient standard is the possibility of a small difference between the temperature measured by the thermometer and the actual temperature of the load in the standard, due to imperfect thermal contact and thermal gradients. This contribution should be similar to that in the waveguide ambient standards. We therefore take the uncertainty in the temperature of the ambient standard to be the same as in the waveguide case,  $u_{T_a} = 0.1$  K,  $\mathcal{E}_{T_a} = 0.034$  percent.

## 4.3 Power Ratios

In the waveguide section above, we concluded that this contribution is negligible. Power measurements are done in the same way for coaxial calibrations as for waveguide calibrations, and so  $u_{T_x}(Y)$  is again negligible.

## 4.4 Mismatch Factors

As in the waveguide case, Subsection 3.4,

$$\frac{u_{T_x}(M/M)}{T_x} = \left| 1 - \frac{T_a}{T_x} \right| \mathcal{E}_{M/M} \approx \left| 1 - \frac{T_a}{T_x} \right| u_{M/M}. \quad (50)$$

The mismatch uncertainty depends strongly on the poorly known correlation between uncertainties in the measurements of different reflection coefficients and again we will use the maximum of the uncertainties obtained by assuming complete correlation and no correlation whatsoever,

$$u_{MM} = \text{Max} \{u_{cor}, u_{uncor}\}. \quad (51)$$

As above, the correlated and uncorrelated uncertainties are given by

$$u_{MM}(cor.) = 4 u_{Im\Gamma} |y_S + y_{r,S} - y_x - y_{r,x}|, \quad (52)$$

$$u_{MM}(uncor.) = 2 \sqrt{2} u_{Re\Gamma} [(x_S - x_{r,S})^2 + (y_S + y_{r,S})^2 + (x_x - x_{r,x})^2 + (y_x + y_{r,x})^2]^{\frac{1}{2}}, \quad (53)$$

where  $x$  and  $y$  refer to real and imaginary parts of the corresponding reflection coefficients. The question then is what is  $u_{Re\Gamma}$ ? References [2] and [4] use  $\pm 0.005$  for the worst-case error in the real or imaginary part. Comparison of reflection-coefficient measurements on our system to those made by the NIST Network Analysis and Measurements Project on the same devices indicated agreement within about  $\pm 0.002$ . Our year-to-year variations in measurements on the same device are well within  $\pm 0.005$ . In the system calibration, we require that the reflection coefficient of the check standards agree with historical values within  $\pm 0.0025$ . These facts lead to the conclusion that  $0.005$  represents a conservative estimate of our worst-case error, and we therefore use half that for the standard uncertainty in real and imaginary parts of reflection coefficients,

$$u_{Re\Gamma} = u_{Im\Gamma} = 0.0025 \quad (54)$$

for all our coaxial systems.

## 4.5 Asymmetry

The form for this uncertainty is the same as for the waveguide case, eqs (19) and (23) above,

$$\frac{u_{T_x}(\eta/\eta)}{T_x} = \left| 1 - \frac{T_a}{T_x} \right| u_{\eta/\eta}, \quad (55)$$

$$u_{\eta/\eta} \approx 0.4 u_{\text{Re}\Gamma}. \quad (56)$$

From the preceding subsection  $u_{\text{Re}\Gamma} = 0.0025$ , and so

$$\frac{u_{T_x}(\eta/\eta)}{T_x} = \left| 1 - \frac{T_a}{T_x} \right| \times 0.1\%. \quad (57)$$

## 4.6 Connector

As in the waveguide case of Subsection 3.6 above, this uncertainty arises from variability from one connector to another of the same type. This variability affects the measurement of the asymmetry, which is measured by measuring the powers from two check standards connected to the DUT port and the cryogenic-standard port, and then switching the two check standards and comparing the measured powers [2,4]. For our coaxial calibrations, the DUT reference plane is located between the DUT and the connector, and similarly the cryogenic-standard reference plane is between the standard and the connector. Thus the connectors are part of the two paths being compared. Any difference in the connection of DUT to the test port and the connection of the check standard to the test port, or between the connection of the cryogenic standard and the connection of the check standard, will result in a difference between the measured asymmetry and the actual asymmetry occurring during the measurement of the DUT.

To estimate the variability from one connector to another of the same type, we turn to results of an Automated RF Techniques Group (ARFTG) comparison conducted by NIST [16]. In this comparison several devices for each connector type were measured at NIST and at a number of different industry laboratories. Each laboratory measured  $S_{11}$  and  $S_{12}$  for each device, and the standard deviations of the samples were computed. The variations observed in this comparison are due to a number of factors, such as differences between the methods and equipment at the laboratories, as well as differences between the connectors on the cables used by the laboratories. Thus the standard deviations observed in reference [16] represent a very conservative estimate of connector variability. The particular results we use are those for the 20-dB attenuator for each connector, computed from the trimmed data (outliers excluded). We expect the variability to increase roughly as  $f^2$ . Taking into account the fact that the results of reference [16] represent maximum values over the stated frequency ranges, we infer the following parameterizations of the connector variabilities (in the *square* of  $|S_{12}|$ ):

$$\sigma_{Conn} \approx \begin{array}{l} 0.00053 \sqrt{f} \text{ GPC-7} \\ 0.00066 \sqrt{f} \text{ Type N} \\ 0.00062 \sqrt{f} \text{ 3.5 mm,} \end{array} \quad (58)$$

where  $f$  is in GHz. Because the devices measured were two-port devices, the results of eq (58) represent the variations from *two* connectors. Since there are two relevant connections in the radiometer measurements, eq (58) can be used directly, resulting in

$$\frac{u_{T_x}(Conn)}{T_x} = \sigma_{Conn} \left| 1 - \frac{T_a}{T_x} \right|. \quad (59)$$

Besides the connectors of eq (58), we also calibrate noise sources with 14-mm connectors, which were not treated in reference [16]. For them we shall use the GPC-7 numbers.

#### 4.7 Isolation

This contribution has the same general form as the waveguide case, provided that the isolation of the radiometer is the same. All the NIST coaxial systems have isolation of at least 40 dB. Measurement of the 8 GHz to 12 GHz system indicated that its isolation exceeds 50 dB across its entire frequency range. We shall therefore use

$$\frac{u_{T_x}(isol)}{T_x} = 0.01 \times \left\{ 0.24 |\Gamma_S| \left| 1 - \frac{T_a}{T_x} \right| + 0.024 \left| 1 - \frac{T_S}{T_x} \right| + 54 \frac{|\Gamma_x|}{T_x} \right\} \quad (60)$$

for the 8GHz to 12 GHz system and

$$\frac{u_{T_x}(isol)}{T_x} = 0.01 \times \left\{ 0.8 |\Gamma_S| \left| 1 - \frac{T_a}{T_x} \right| + 0.08 \left| 1 - \frac{T_S}{T_x} \right| + 180 \frac{|\Gamma_x|}{T_x} \right\} \quad (61)$$

for 1 GHz to 8 GHz, where  $T_x$  is in kelvins.

#### 4.8 Frequency Offset (Broadband Mismatch)

The form of this uncertainty is the same as for the waveguide case,

$$\begin{aligned} \frac{u_{T_x}(BBMM)}{T_x} &= \frac{200\%}{\sqrt{3}} \left| \cos\left(\frac{4 \pi f_{IF} l}{30}\right) \text{sinc}\left(\frac{\pi B l}{15}\right) - 1 \right| \\ &\times (|\Gamma_S \Gamma_{r,S}| + |\Gamma_x \Gamma_{r,x}|) \left| 1 - \frac{T_a}{T_x} \right|, \end{aligned} \quad (62)$$

except that the electrical length  $l_e$  has reverted to the physical length  $l$ , and the parameters  $f_{IF}$ ,  $B$ , and  $l$  are different. The values of the system parameters are given in Table 4. The IF frequency refers to the offset between the measurement frequency and the center of the pass band. The bandwidth (for  $f_{IF} = 0$ ) is the full detection bandwidth, which is twice the bandwidth of the IF filter.

Table 4. Coaxial system parameters for use in eq (62).

System	$f_{IF}$ (GHz)	$B$ (GHz)	$l$ (cm)
1-2 GHz	0	0.010	116.
2-4 GHz	0	0.010	72.
4-8 GHz	0	0.010	76.
8-12 GHz	0	0.010	61.

#### 4.9 Nonlinearity

The final type-B source of uncertainty in the DUT noise temperature is nonlinearity of the system. For coaxial calibrations, system linearity is tested during each noise-temperature measurement. Twenty five readings are taken with a 3-dB attenuator in the IF section of the system, and 25 readings are taken without the attenuator. The two resulting noise temperatures must agree within 0.2 percent. Using the same analysis as in Subsection 3.9 above, this translates into

$$\frac{u_{T_x}(lin)}{T_x} = 0.10\% . \quad (63)$$

#### 4.10 Type-A and Combined Uncertainties

For calibrations using the coaxial systems, the system six-port reflectometer is calibrated just once, and the DUT is disconnected and remeasured several times on two different measurement ports. The type-B standard uncertainty is essentially the same for each of the measurements and is obtained by forming the square root of the sum of the squares of the individual contributions eqs (46, 49, 50, 57, 59, 60 or 61, 62, 63),

$$u_B = [u_{T_x}^2(Cry) + u_{T_x}^2(amb) + u_{T_x}^2(Y) + u_{T_x}^2(M/M) + u_{T_x}^2(\eta/\eta) + u_{T_x}^2(isol) + u_{T_x}^2(con) + u_{T_x}^2(BBMM) + u_{T_x}^2(lin)]^{1/2}. \quad (64)$$

The type-A standard uncertainty is just the standard deviation of the mean of the different measurements,

$$u_A = \sqrt{\frac{\sum (\bar{T}_x - T_{x,i})^2}{N(N-1)}}, \quad (65)$$

and the expanded uncertainty is twice the combined standard uncertainty,

$$U_{T_x} = 2 \sqrt{u_{T_x,A}^2 + u_{T_x,B}^2}. \quad (66)$$

## 5. OTHER SYSTEMS

### 5.1 WR-90 (8 GHz to 12.4 GHz) Switching Radiometer

For the WR-90 band, a switching, or Dicke [5], radiometer is used [6]. The quantity measured with this system is the effective noise temperature delivered to a reflectionless load ( $T_{ne}$ ). It is related to the *available* noise temperature  $T$ , which is measured by all the other systems, by

$$T_{ne} = (1 - |\Gamma|^2) T, \quad (67)$$

where  $\Gamma$  is the reflection coefficient of the noise source. The current uncertainty analysis uses the original analysis [6] as a starting point. Five sources of uncertainty were identified initially, and a sixth was added later. The five original components were due to the effective noise temperature  $T_{ne,S}$  of the working standard, the temperature  $T_A$  of the precision attenuator, the attenuation difference  $D$  between the standard and unknown noise sources as measured

with the precision attenuator, the measurement of the reflection coefficients  $\Gamma$  using a tuned reflectometer, and the determination of the mismatch factor  $M$ . The later addition was the uncertainty in the loss in the waveguide flange. The original analysis took the maximum values of the five separate uncertainties and added them linearly to obtain a worst-case error. We take each of the five maximum contributions and divide by 2 to obtain a standard uncertainty, yielding

$$\begin{aligned}
 u(Std) &= 10^{D/10} \frac{\Delta T_{ne,S}}{2}, \\
 u(D) &= 0.23(T_{ne} - T_A) \frac{\Delta D}{2}, \\
 u(T_A) &= (1 - 10^{D/10}) \frac{\Delta T_A}{2}, \\
 u(\Gamma) &= T_A (10^{D/10} |\Gamma_S|^2 + |\Gamma_x|^2) \frac{\Delta \Gamma_S}{|\Gamma_S|}, \\
 u(M) &= \frac{1}{2} \left[ \frac{(1 + |S_{11} \Gamma_x|)^2}{(1 - |S_{11} \Gamma_x|)^2} - 1 \right] [T_{ne} - T_A (1 - |\Gamma_x|^2)],
 \end{aligned} \tag{68}$$

where the subscript  $S$  refers to the standard, and  $x$  refers to the DUT. The worst-case error in the noise temperature of the working standard depends on frequency and the particular standard used; it is typically around 100 K out of a noise temperature of the order of  $10^4$  K. The worst-case error in  $D$  is  $\Delta D = 0.006$  or  $0.008$ , depending on the settings of the attenuator. Values of the other parameters appearing in eq (68) are

$$|S_{11}| = 0.01, \quad \Delta T_A = 2 \text{ K}, \quad \frac{\Delta \Gamma}{\Gamma} = 0.1. \tag{69}$$

The contribution from the uncertainty in the flange loss is given approximately by

$$u(Fl) = \frac{1}{2} (10^{\frac{\Delta Fl}{10}} - 1) (T_S - T_A) (1 - |\Gamma_S|^2) 10^{\frac{D}{10}}, \tag{70}$$

with  $\Delta FI = 0.005$ . The type-B uncertainty in the measured effective noise temperature is then

$$u_B = \sqrt{u(Std)^2 + u(D)^2 + u(T_A)^2 + u(\Gamma)^2 + u(M)^2 + u(FI)^2}. \quad (71)$$

There are two type-A uncertainties. The noise temperatures of the working standards were measured several times against the primary (oven) standard [17]. The resulting contribution to the uncertainty in  $T_{ne}$  of the DUT is

$$u_{A,1} = 10^{\frac{D}{10}} u_{A,S}, \quad (72)$$

where  $u_{A,S}$  is the standard deviation of the mean of the measurements of the noise temperature of the working standard. In measuring the noise temperature of an unknown device, five separate measurements of its noise temperature are made and averaged. The standard deviation of the mean of these five measurements is the other type-A uncertainty,  $u_{A,2}$ . The full type-A uncertainty is then

$$u_A = \sqrt{u_{A,1}^2 + u_{A,2}^2}, \quad (73)$$

and the expanded uncertainty quoted in calibration reports is

$$U = 2\sqrt{u_A^2 + u_B^2}, \quad (74)$$

with  $u_A$  and  $u_B$  given by eqs (71) and (73).

## 5.2 Tuned Systems for 30 and 60 MHz

At 30 MHz and 60 MHz, noise temperature is measured on an unisolated radiometer, using tunable standards [1]. The original estimation of the individual components of uncertainty is still used, with two exceptions. The uncertainty in the temperature of the ambient standard has been converted to a standard uncertainty by assuming a uniform

distribution and dividing by  $\sqrt{3}$ , and the uncertainty in the power ratio is now negligible, as discussed in Subsection 3.3 above. For the other components—the cryogenic standard, the mismatch factor, the nonlinearity, switch asymmetry, and the adapter (when present)—the original values from reference [1] and the associated computer program are still used. The type-A uncertainty is the standard deviation of the mean of the independent measurements, and the individual components are added in quadrature to obtain the combined uncertainty.

## 6. MEASUREMENTS THROUGH ADAPTERS

### 6.1 Background

In certain frequency ranges and for certain connectors, the noise temperature calibrations are performed through adapters. In such cases, we measure the noise temperature of the device-adapter combination, and we must then correct for the effect of the adapter in order to determine the noise temperature of the device alone. Referring to fig. 2, we can write

$$T_2 = T_{x+a} = \alpha_{21} T_x + (1 - \alpha_{21}) T_a, \quad (75)$$

$$T_x = \frac{T_{x+a} - (1 - \alpha_{21}) T_a}{\alpha_{21}},$$

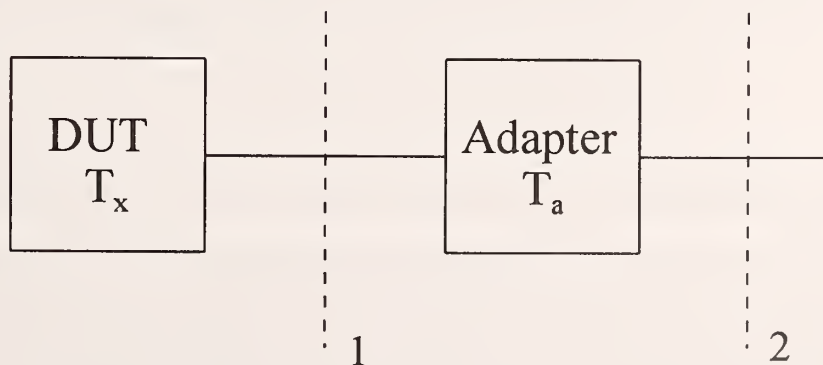


Figure 2. Reference planes for a noise source with an adapter.

where  $\alpha_{21}$  is the available power ratio,  $\alpha_{21} \equiv p_2^{avail}/p_1^{avail}$ , and where the adapter is assumed to be at ambient temperature, with noise temperature  $T_a$ . Thus, if we can determine  $\alpha_{21}$ , we can compute the device temperature  $T_x$  from the device-adapter temperature  $T_{x+a}$ . To determine  $\alpha_{21}$ , we follow Engen [18] in noting that  $\alpha_{21} = \eta_{12}$ , where  $\eta_{12}$  is the efficiency,  $\eta_{21} \equiv p_2^{del}/p_1^{del}$ . For reciprocal devices  $\eta_{12} = \eta_{21}$ , and so  $\alpha_{21} = \eta_{21}$  for reciprocal devices. We then use Daywitt's method [19,20] to measure  $\eta_{21}$ .

We need not reproduce the algebra, but there are two key equations needed from reference [20]. The first approximates the efficiency as the intrinsic efficiency for a low-loss, well matched device,

$$\begin{aligned}\eta_{21} &\approx \eta_{21_0} [1 + 2 \operatorname{Re}(\chi \Gamma)], \\ \chi &\approx S_{22} (1 - \eta_{21_0}),\end{aligned}\tag{76}$$

where  $\Gamma_1$  is the reflection coefficient of the load under "normal" use (the radiometer in our case), and  $\eta_{21_0}$  is the intrinsic efficiency of the adapter,  $\eta_{21_0} = |S_{21}|^2/(1 - |S_{11}|^2)$ . Since both  $\chi$  and  $\Gamma_1$  are small, eq (76) is used to justify the approximation  $\eta_{21} \approx \eta_{21_0}$ . The other key equation relates the intrinsic efficiency to the reflection coefficient  $\Gamma_2$  from the adapter at plane 2 when the adapter is terminated with a low-loss reflective termination at plane 1,

$$|\Gamma_2| \approx \eta_{21_0} |\Gamma_r| - |\chi| \cos \phi,\tag{77}$$

where  $\Gamma_r$  is the reflection coefficient of the reflective termination ( $\approx 1$ ), and  $\phi$  is a phase angle which varies (approximately) linearly and relatively rapidly (compared to  $\eta_{21_0}$ ) with frequency. Equation (77) indicates that  $|\Gamma_2|$  consists of a rapidly varying piece, due to the second term on the right side, superimposed on a more slowly varying piece due to the  $\eta_{21_0}$  term. The idea then is to measure  $|\Gamma_2|$  and smooth out the oscillations in frequency. That

should yield  $\eta_{21_0} |\Gamma_r|$ , which can be divided by  $|\Gamma_r|$  to yield the desired quantity. For a good flush short  $|\Gamma_r|$  can be taken to be 1, but for an offset short or offset open a correction is usually required to account for the loss in the small length of line constituting the offset.

The process of smoothing the oscillations in frequency is facilitated by measuring  $|\Gamma_2|$  with two different reflective terminations, whose reflection coefficients differ in phase by  $\pi$ . Typical choices would be a flush short and an offset short for a waveguide port, or an offset open and an offset short for a coaxial port. As an example, we consider evaluation of an adapter from 3.5-mm coaxial line to WR-42 waveguide. Referring to fig. 2, we identify port 1 with the 3.5-mm port and port 2 with the WR-42 port. We measured  $|\Gamma_2|$ , the reflection coefficient from port 2, when port 1 was terminated with two different reflective loads, in this case an offset open and an offset short. The offset refers to a short length of transmission line before the open or short. The open for the coaxial line is achieved by truncating the inner conductor, replacing it with a length of dielectric of equal radius, while the outer conductor is continued to provide shielding. The results are shown in fig. 3. Each curve is approximately what would be expected from eq (77), regular oscillations ( $\chi \cos\phi$ ) on a smooth overall frequency dependence ( $\eta_{21_0} |\Gamma_r|$ ). The smaller wiggles on the large waves are attributable to VNA imperfections.

There could be some question of how we know that the larger waves, which we attribute to  $\chi \cos\phi$ , are not due instead to VNA errors. By comparing the respective magnitudes of  $\chi$  and VNA uncertainties to the size of the oscillations, we can argue that the oscillations are due primarily to the expected  $\chi \cos\phi$  term; but there is also more direct, compelling, experimental evidence. Figure 4 shows results of measurements of  $|\Gamma_2|$  made first on an adapter with two different reflective terminations and then on the same adapter and terminations with a 3.5-cm length of line inserted between the adapter and the termination. The wavelength (in frequency) of the large oscillations becomes much shorter when the line is introduced, indicating that these waves are due to the device rather than to the VNA. (We will revisit this point in the uncertainty analysis section below.)

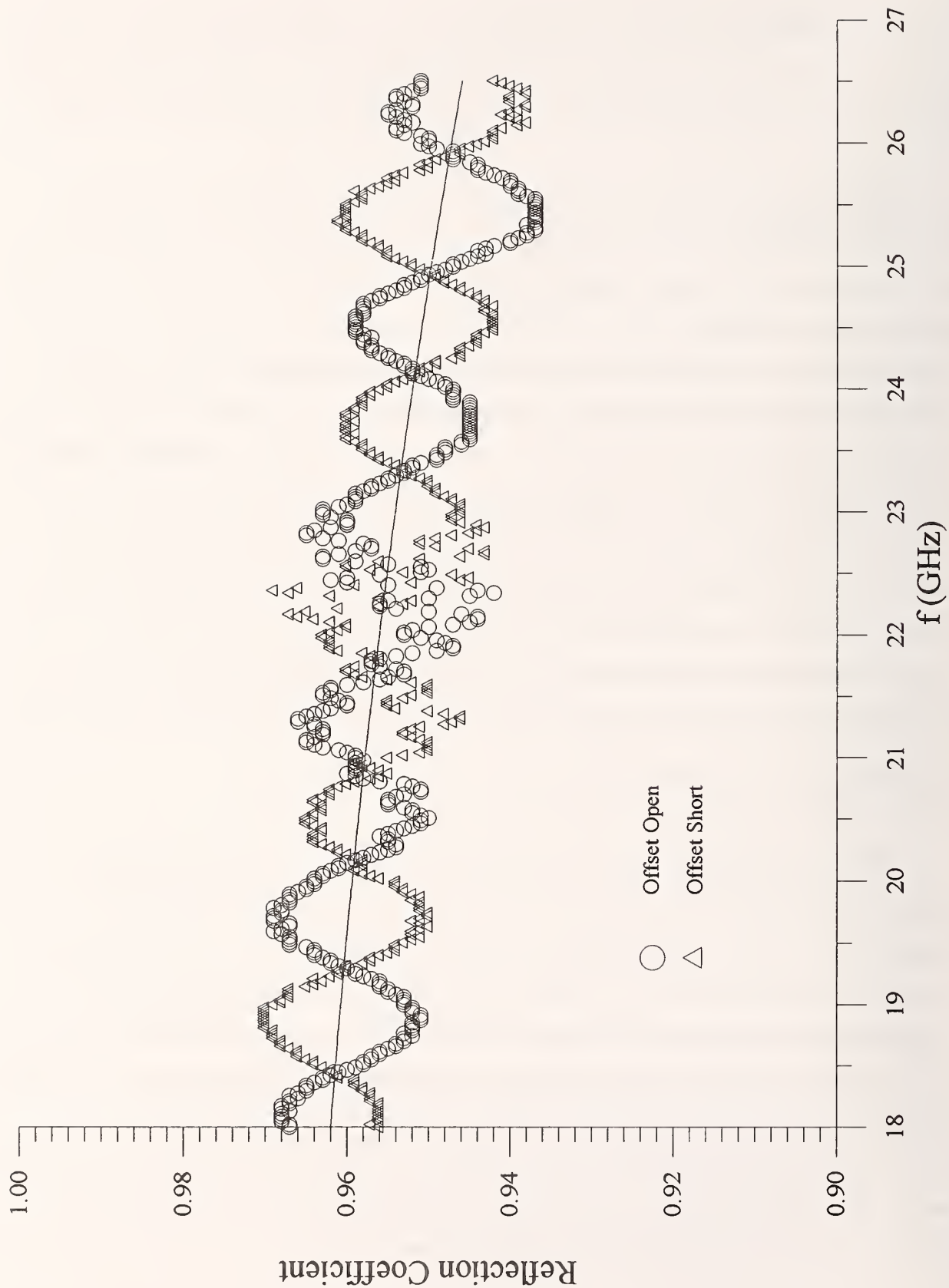


Figure 3. Measured reflection coefficient of 3.5-mm to WR-42 adapter with reflective terminations.

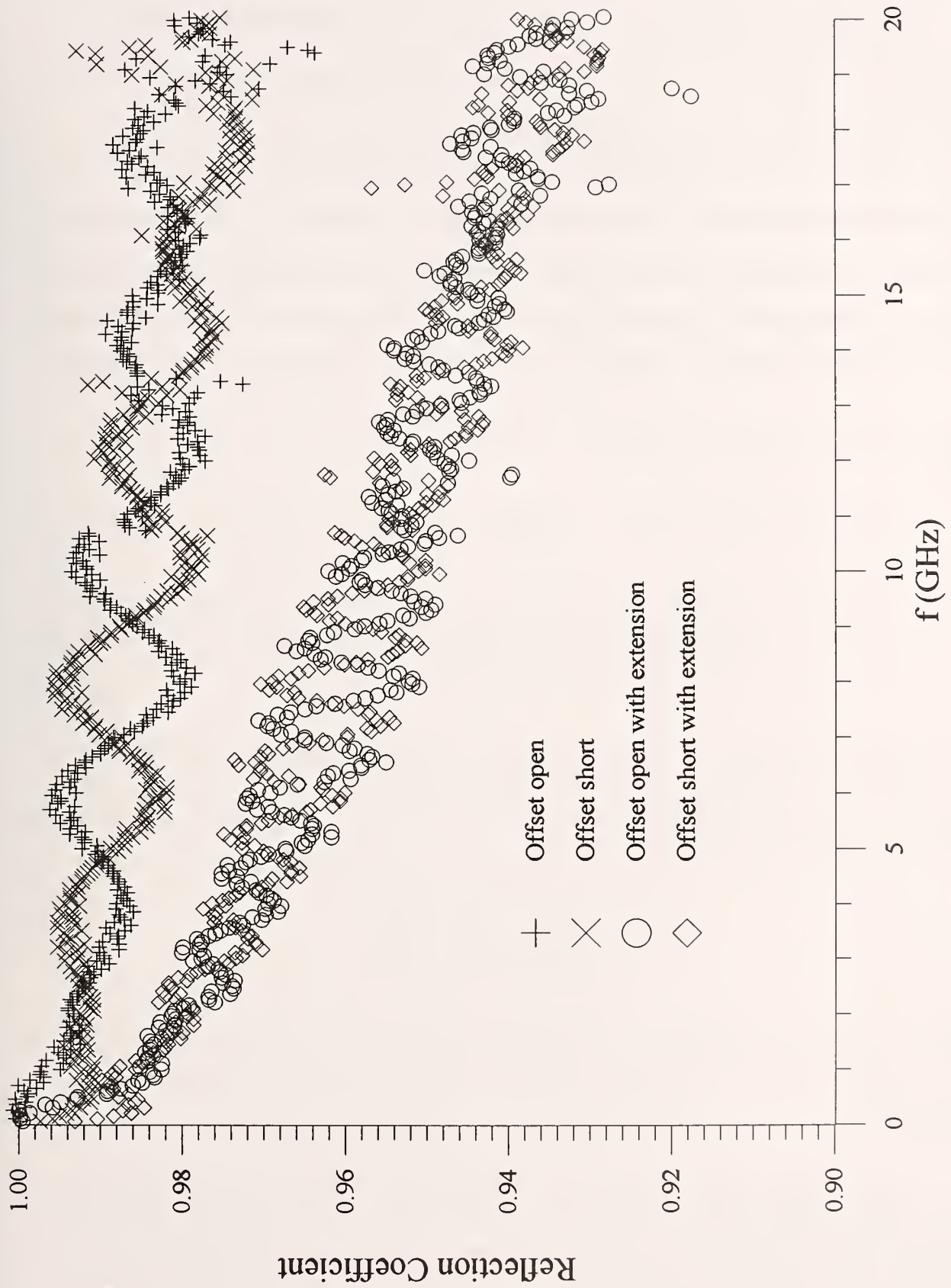


Figure 4. Measured reflection coefficients from adapter (3.5 mm to type N) with reflective terminations, with (lower pair) and without (upper pair) 3.5 cm line.

Returning to the determination of  $\eta_{21_0}$ , at present we do the smoothing in fig. 3 by hand, simply by drawing a smooth curve corresponding to an average of the sinusoids. As pointed out in reference [20], it should be sufficient to use just one of the experimental curves, but in this case the smoothed curves from the two sinusoids coincide. From eq (77) we see that the smoothed curve corresponds to  $\eta_{21_0} |\Gamma_r|$ . Numerical values can be read off the graph. To obtain the intrinsic efficiency we divide by  $|\Gamma_r|$ , the reflection coefficient of the reflective termination. For the case shown here,  $|\Gamma_r|$  was calculated from data provided by the manufacturer, with the result that  $|\Gamma_r| = 0.9965$  at 18 GHz and 0.996 at 26.5 GHz.

## 6.2 Uncertainty Analysis

Starting with the second form of eq (75) and taking small variations of both sides, we obtain

$$\delta T_x = \frac{1}{\alpha} \delta T_{x+a} - \left( \frac{1}{\alpha} - 1 \right) \delta T_a + (T_x - T_a) \frac{\delta \alpha}{\alpha}. \quad (78)$$

In principle,  $\delta T_{x+a}$  and  $\delta T_a$  are correlated since  $\delta T_{x+a}$  contains a contribution from the uncertainty in the ambient temperature. In practice, however, the  $\delta T_a$  term in eq (78) is negligible (roughly 0.01 K), and we will use

$$u_x = \sqrt{\frac{u_{x+a}^2}{\alpha^2} + (T_x - T_a)^2 \frac{u_\alpha^2}{\alpha^2}}. \quad (79)$$

The  $u_{x+a}$  is the standard uncertainty in the measurement of the device-plus-adapter, evaluated as in Section 3 or 4 above. The problem is to evaluate  $u_\alpha$  when  $\alpha$  is determined by the method described in the preceding subsection.

There are four major components to  $u_\alpha$ : the uncertainty associated with determining  $\eta_{21_0}$  from the measured  $|\Gamma_2|$ , the VNA uncertainty associated with the measurement of

$|\Gamma_2|$ , the uncertainty introduced by the approximation  $\eta_{21} \approx \eta_{21_0}$ , and the uncertainty introduced by connector repeatability (or lack thereof).

The determination of  $\eta_{21_0}$  from the graph can contain both type-A and type-B uncertainties. The type-A uncertainty arises from the fact that in effect we have two quasi-independent measurements of  $\eta_{21_0}$ , arising from the measurements with the two different reflective terminations. If we denote the two smoothed curves as  $\eta_1$  and  $\eta_2$ , this contribution is given by

$$u_{1,A}^2 = \frac{1}{2 \times 1} [(\bar{\eta} - \eta_1)^2 + (\bar{\eta} - \eta_2)^2], \quad (80)$$

$$\bar{\eta} = \frac{\eta_1 + \eta_2}{2}.$$

In principle,  $u_{1,A}$  varies with frequency, but in practice we use the value at the point of maximum separation between  $\eta_1$  and  $\eta_2$ . In the example considered above, this contribution is negligible.

The type-B part of this contribution to the uncertainty arises from the uncertainty in determining the appropriately smoothed curve for each of the measured  $|\Gamma_2|$  curves. The uncertainty in drawing the smoothed curve is about 0.002 in typical cases, such as that of fig. 3, leading to

$$\delta_{1,B} = \frac{\delta\eta_1 + \delta\eta_2}{2}, \quad (81)$$

$$u_{1,B}^2 = \frac{(0.002)^2}{4} + \frac{(0.002)^2}{4} = 2 \times 10^{-6}.$$

Combining the type-A and type-B uncertainties for the present example results in  $u_1 = u_{1,B} = 0.0014$ .

The second source of uncertainty is the VNA measurement of  $|\Gamma_2|$ , for which we use the uncertainties provided by the manufacturer. The manufacturer does not quote uncertainties for one-port measurements, and so we use the values for the uncertainty in  $|S_{11}|$  in two-port measurements. This should represent an overestimate of our actual one-port uncertainties since the two-port uncertainties include the effect of cables, which are not used in our measurements of the reflection coefficient. In addition, our smoothing procedure may eliminate part of the VNA calibration error. However, since we do not have a good way of estimating how much we have improved the VNA uncertainty, we will just use the full values given by the manufacturer. These values depend strongly on the connector type and also depend on the frequency and on the magnitude of the reflection coefficient being measured. The relevant connector type for us is the connector at plane 2 (WR-42 in the example), since that is where we are making the VNA measurement. The standard uncertainty for WR-42 is

$$u_2 = 0.0025. \quad (82)$$

From the smoothing of the measured curves for  $|\Gamma_2|$  we obtain the intrinsic efficiency  $\eta_{21_0}$ , which we then use as an approximation to the efficiency  $\eta_{21}$ , eq (76). The term we neglect has a maximum magnitude of  $|2\chi\Gamma_1|$ . We do not know the relative phase of  $\chi$  and  $\Gamma_1$ , and so we assume the correction term has a uniform probability to assume any value between plus and minus its maximum magnitude. We can estimate this magnitude by noting that  $\Gamma_1$  is the reflection coefficient of the normal load, the radiometer. For WR-42,  $|\Gamma_1| \leq 0.1$ . The magnitude of  $\chi$  can be estimated from the magnitude of the large oscillations in the graphs of  $|\Gamma_2|$ , using eq (77). From fig. 3 we estimate that  $|\chi|$  is about .0035 for the present adapter. Consequently, the neglected term has a maximum magnitude of about 0.00085. Dividing by  $\sqrt{3}$  to obtain the standard uncertainty, we have  $u_3 = 0.005$ . As an aside we note that we can also check the effect of neglecting the imaginary part of  $\chi\Gamma_1$  in obtaining eq (76). The effect is entirely negligible ( $\sim 10^{-6}$ ), as expected.

Finally, there is the issue of connector repeatability. The uncertainty due to the nonrepeatability of the connector at port 2 is included in the VNA uncertainty. The connector

at port 1 is 3.5-mm coaxial in our example. A recent comparison by the NIST Network Analysis and Measurements Project achieved a repeatability of about 0.0003 with 3.5-mm connectors. We will use a more conservative value of 0.001, which is also approximately consistent with the experience of our technicians,

$$u_4 = 0.001 \quad (3.5\text{-mm connector}). \quad (83)$$

The combined standard uncertainty for  $\alpha$  is obtained by adding the four individual components in quadrature, with the result

$$\begin{aligned} u_\alpha &= \sqrt{u_1^2 + u_2^2 + u_3^2 + u_4^2}, \\ &= 0.003. \end{aligned} \quad (84)$$

This value is then used in eq (79) to compute the standard uncertainty in the determination of  $T_x$ . Typical values for  $u_\alpha$  range from 0.003 to 0.006. In a typical calibration, the use of an adapter increases the expanded uncertainty by a few tenths of a percent or less for frequencies up to 26 GHz.

## 7. SUMMARY

The uncertainty analyses for all the NIST noise-temperature calibration systems were presented, including calibrations made through adapters. Although many of the individual components had been evaluated previously, some had not been, and many were reevaluated, corrected, or converted from worst-case errors to standard uncertainties. In some cases, previously scattered treatments were integrated and, when necessary, reconciled. In all cases, the uncertainty analysis is now consistent with the CIPM guidelines [7,8]. Typical expanded ( $k = 2$ ) uncertainties in the measured noise temperature are in the range 0.7 percent to 1.4 percent, depending on the particular system and the frequency.

---

Much of the content of this paper is the direct or indirect product of numerous conversations with former members of the NIST Noise Project, in particular Bill Daywitt, Jack Rice, and Dave Wait. I am also grateful to Bob Jewish for discussions about statistical methods and to John Juroshek for discussions about VNA and six-port measurements and connectors.

## 8. REFERENCES

- [1] Counas, G.J., and Bremer, T.H. NBS 30/60 megahertz noise measurement system operation and service manual. Nat. Bur. Stand. (U.S.) Interagency Report 81-1656; 1981 December.
- [2] Daywitt, W.C. Radiometer equation and analysis of systematic errors for the NIST automated radiometers. Natl. Inst. Stand. Technol. Tech. Note 1327; 1989 March.
- [3] Counas, G.J. 2.0 GHz to 4.0 GHz automated radiometer operation and service manual. Nat. Bur. Stand. (U.S.) Interagency Rep. 83-1697; 1984 January.
- [4] Randa, J.; Terrell, L.A. NIST WR-28 noise-temperature measurement system. Natl. Inst. Stand. Technol. Tech. Note 1395; 1997 August.
- [5] Dicke, R.H. The measurement of thermal radiation at microwave frequencies. Rev. Sci. Instrum. 17(7): 268-275; 1946 July.
- [6] Miller, C.K.S.; Daywitt, W.C. The NBS switching radiometers. Nat. Bur. Stand. (U.S.) Interagency Rep. 84-3004; 1984 May.

- [7] ISO Guide to the Expression of Uncertainty in Measurement. International Organization for Standardization; Geneva, Switzerland; 1993.
- [8] Taylor, B.N.; Kuyatt, C.E. Guidelines for evaluating and expressing the uncertainty of NIST measurement results. Natl. Inst. Stand. Technol. Tech. Note 1297, 1994 edition; 1994 September.
- [9] Daywitt, W.C. A derivation for the noise temperature of a horn-type noise standard. Metrologia 21: 127-133; 1985.
- [10] Pucic, S.P. The uncertainty in Y-factor measurements. URSI National Radio Science Meeting Digest; Boulder, CO; 1995. p. 39.
- [11] Pucic, S.P. Uncertainties of the NIST coaxial noise calibration system. Conference on Precision Electromagnetic Measurements Digest; Boulder, CO; 1994. 254-255.
- [12] Pucic, S.P. Broadband mismatch error in noise measurement systems. Conference on Precision Electromagnetic Measurements Digest; Paris; 1992. 256-257.
- [13] Graybill, F.A. Theory and Application of the Linear Model. Duxbury Press; Belmont, CA; 1976.
- [14] Daywitt, W.C. A new reference grade coaxial thermal noise standard for the 10 MHz to 18 GHz frequency range. Submitted to IEEE Trans. Microwave Theory Tech, 1997.
- [15] Daywitt, W.C. A coaxial noise standard for the 1 GHz to 12.4 GHz frequency range. Nat. Bur. Stand. (U.S.) Tech. Note 1074; 1984 March.
- [16] Juroshek, J; Ondrejka, C; Judish, R.; Vecchia, D; and Splett, J. Preliminary analysis of ARFTG measurement comparison program. NIST-ARFTG Short Course; Boulder,

CO; 1994 November.

- [17] Miller, C.K.S, and Daywitt, W.C. The NBS WR62 and WR90 reference noise standards. Nat. Bur. Stand. (U.S.) Interagency Report 884-3005; 1984 May.
- [18] Engen, G.F. A method of calibrating coaxial noise sources in terms of a waveguide standard. IEEE Trans. MTT-16(9): 636-639; 1968 September.
- [19] Daywitt, W.C. Determining adapter efficiency by envelope averaging swept frequency reflection data. IEEE Trans. MTT-38(11): 1748-1752; 1990 November.
- [20] Pucic, S.P., and Daywitt, W.C. Single-port technique for adapter efficiency evaluation. 45th ARFTG Conference Digest, Orlando, FL, May 1995, pp. 113-118; 1995.

## APPENDIX

The question is how to estimate the type-B standard uncertainty when we already know a "worst-case error." The reason this is a problem at all is that worst-case errors do not translate directly into the CIPM/ISO scheme, which is based on standard deviations. To relate the two we must inject additional information, either explicitly or implicitly (for example, by the distribution used in whatever method we employ). In choosing a particular conversion method, we shall be guided by two general principles (besides technical validity):

1. In providing the additional information required, it is better to use even qualitative knowledge rather than to rely on uneducated guesses or arbitrary choices. If estimates or best guesses are required, it is preferable to estimate quantities about which we have some knowledge or intuition.
2. The bottom line is the expanded uncertainty, which should reflect a 95 percent confidence level. That is what we provide to our measurement services customers.

We should choose a method for estimating type-B uncertainties which produces an expanded uncertainty that best reflects our knowledge of the measurement uncertainties.

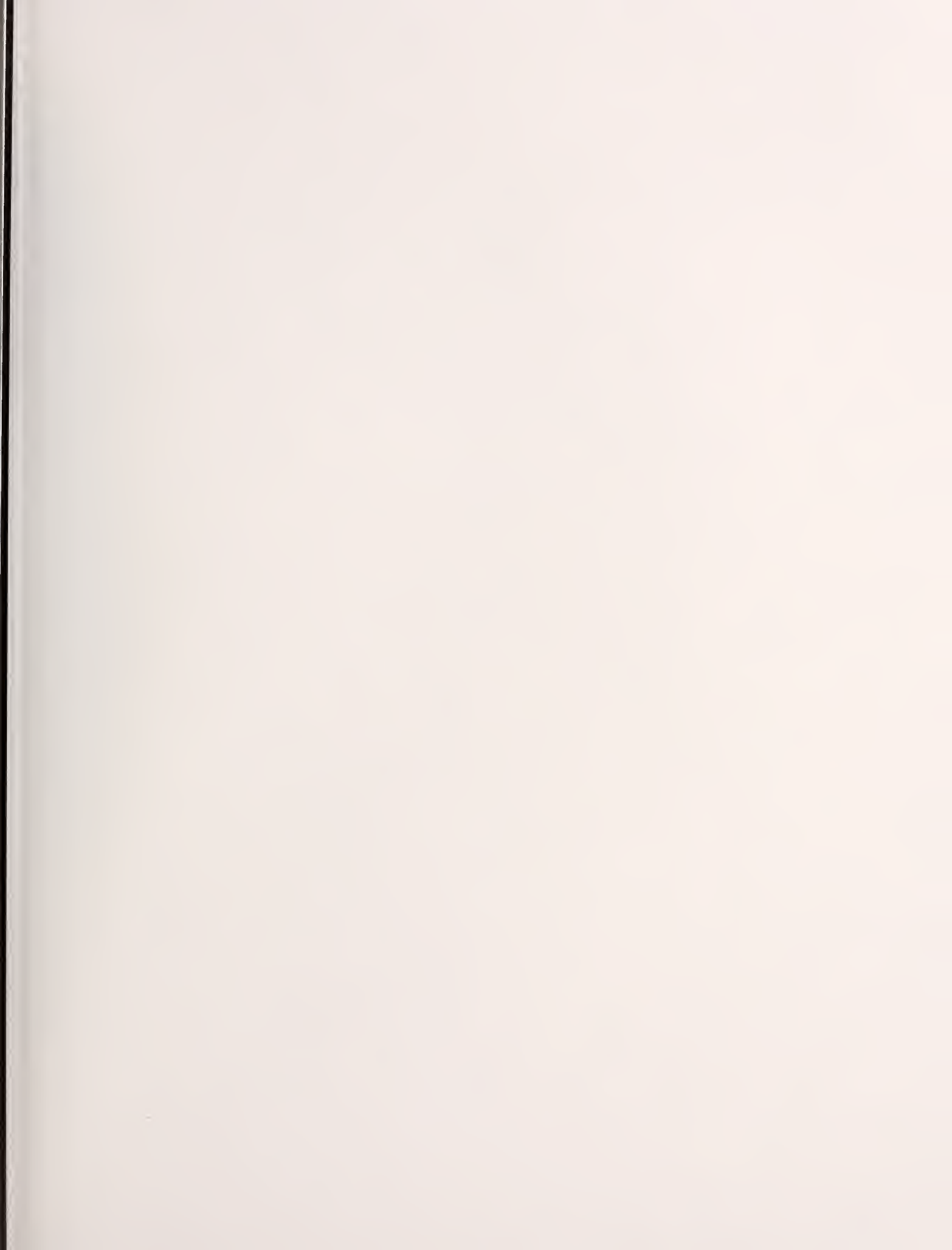
In its Section 4, reference [8] provides a number of ways to estimate type-B uncertainties. Most of the methods consist of choosing a statistical distribution (normal, rectangular, triangular) to model the quantity in question and then estimating the likelihood that the true value of the quantity lies within some chosen interval of the estimated value of the quantity (typically the mid-point of the interval, the average value). The standard uncertainty is then obtained by determining the standard deviation for the chosen distribution in terms of the estimated likelihood in the chosen interval. The case of estimating the standard uncertainty when a worst-case error is known is addressed in Subsection 4.6. The simplest course of action would be to blindly apply the method of 4.6, which does seem to be in widespread use. There are some undesirable features of that method, however.

Suppose we are interested in a quantity  $A$ , and our best estimate of its value is  $a$ , and the worst-case error is  $\Delta a$ , that is, for all practical purposes the probability is 100 percent that the true value is between  $a - \Delta a$  and  $a + \Delta a$ . Then subsection 4.6 suggests that  $A$  be modeled by a rectangular distribution (equally probable anywhere in the interval  $a \pm \Delta a$ ). This leads to the relation that  $u_a = \sigma = \Delta a / \sqrt{3}$ . One immediate objection is that a rectangular distribution seems a very poor choice. It means that the values at the very edge of the interval are as likely as the values at the center, but that values just beyond the edge have zero probability. That is usually unrealistic. A second, more practical, problem occurs when we compute the expanded uncertainty ( $k = 2$ ), which is supposed to correspond to a 95 percent level of confidence. This results in  $U_a = 2u_a = 2\Delta a / \sqrt{3}$ , which is greater than  $\Delta a$ . That means that before the conversion we were 100% certain that  $A$  was within  $\Delta a$  of  $a$ , whereas now we are only 95 percent confident that  $A$  is within  $1.15 \times \Delta a$  of  $a$ , which is a bigger interval but less confidence! (It is true that  $u$  or  $\Delta a$  is typically just one contribution to the overall uncertainty, but it may be the dominant one, and the other contributions are

subject to the same problem.) This inconsistency occurs in a particularly bad place for measurement services, since the expanded uncertainty is the quantity of most interest; it is what we quote for the customers. Another relevant feature of this approach is the observation made in reference [8] that if we had used a triangular distribution instead of a rectangular distribution, then we would have obtained  $u_a = \Delta a / \sqrt{6}$ , and  $U_a = 2\Delta a / \sqrt{6} < \Delta a$ . This is a useful reminder that in this approach, the choice of the distribution is effectively a choice of the uncertainty (for a given worst-case error).

The fact that the choice of the distribution determines the answer would not be bothersome if we had some good way of choosing the distribution. But if we are quoting a worst-case error we probably don't really know anything about the distribution anyway. A more appropriate approach (for us) is given in Subsection 4.3 of reference [8]. It uses the confidence interval associated with the known uncertainty and assumes a normal distribution (unless there is information to the contrary) to compute a standard deviation and thus the standard uncertainty. If  $\Delta a$  corresponds to a 95 percent confidence interval, then  $u_a = \Delta a / 1.96$ ; if it is a 99 percent confidence interval,  $u_a = \Delta a / 2.576$ . We prefer this approach because we are in a better position to estimate a confidence level associated with the worst-case error than to estimate the distribution. Another advantage is that there is a clear, direct link between the choice we make and the final quantity we are calculating, which is the 95 percent confidence-level uncertainty which we quote to the customer. In the previous method (Subsection 4.6) that link was more obscure.

In practice then, we adopt the following approach. Rather than agonize over exactly how confident we are, we shall use a two-state system. If we are very confident ( $\geq 95$  percent) of the worst-case error, we will use  $u_a = \Delta a / 2$ . This results in an expanded uncertainty  $U_a = \Delta a$ , that is, our uncertainty for 95 percent confidence level is equal to the previous worst-case error. If we are less confident of the worst-case error, we shall continue to use  $u_a = \Delta a / \sqrt{3}$ , which results from a 92 percent confidence level for the worst-case error.





# *NIST* Technical Publications

## *Periodical*

---

**Journal of Research of the National Institute of Standards and Technology**—Reports NIST research and development in those disciplines of the physical and engineering sciences in which the Institute is active. These include physics, chemistry, engineering, mathematics, and computer sciences. Papers cover a broad range of subjects, with major emphasis on measurement methodology and the basic technology underlying standardization. Also included from time to time are survey articles on topics closely related to the Institute's technical and scientific programs. Issued six times a year.

## *Nonperiodicals*

---

**Monographs**—Major contributions to the technical literature on various subjects related to the Institute's scientific and technical activities.

**Handbooks**—Recommended codes of engineering and industrial practice (including safety codes) developed in cooperation with interested industries, professional organizations, and regulatory bodies.

**Special Publications**—Include proceedings of conferences sponsored by NIST, NIST annual reports, and other special publications appropriate to this grouping such as wall charts, pocket cards, and bibliographies.

**Applied Mathematics Series**—Mathematical tables, manuals, and studies of special interest to physicists, engineers, chemists, biologists, mathematicians, computer programmers, and others engaged in scientific and technical work.

**National Standard Reference Data Series**—Provides quantitative data on the physical and chemical properties of materials, compiled from the world's literature and critically evaluated. Developed under a worldwide program coordinated by NIST under the authority of the National Standard Data Act (Public Law 90-396). NOTE: The Journal of Physical and Chemical Reference Data (JPCRD) is published bi-monthly for NIST by the American Chemical Society (ACS) and the American Institute of Physics (AIP). Subscriptions, reprints, and supplements are available from ACS, 1155 Sixteenth St., NW, Washington, DC 20056.

**Building Science Series**—Disseminates technical information developed at the Institute on building materials, components, systems, and whole structures. The series presents research results, test methods, and performance criteria related to the structural and environmental functions and the durability and safety characteristics of building elements and systems.

**Technical Notes**—Studies or reports which are complete in themselves but restrictive in their treatment of a subject. Analogous to monographs but not so comprehensive in scope or definitive in treatment of the subject area. Often serve as a vehicle for final reports of work performed at NIST under the sponsorship of other government agencies.

**Voluntary Product Standards**—Developed under procedures published by the Department of Commerce in Part 10, Title 15, of the Code of Federal Regulations. The standards establish nationally recognized requirements for products, and provide all concerned interests with a basis for common understanding of the characteristics of the products. NIST administers this program in support of the efforts of private-sector standardizing organizations.

**Consumer Information Series**—Practical information, based on NIST research and experience, covering areas of interest to the consumer. Easily understandable language and illustrations provide useful background knowledge for shopping in today's technological marketplace.

Order the **above** NIST publications from: Superintendent of Documents, Government Printing Office, Washington, DC 20402.

Order the **following** NIST publications—FIPS and NISTIRs—from the National Technical Information Service, Springfield, VA 22161.

**Federal Information Processing Standards Publications (FIPS PUB)**—Publications in this series collectively constitute the Federal Information Processing Standards Register. The Register serves as the official source of information in the Federal Government regarding standards issued by NIST pursuant to the Federal Property and Administrative Services Act of 1949 as amended, Public Law 89-306 (79 Stat. 1127), and as implemented by Executive Order 11717 (38 FR 12315, dated May 11, 1973) and Part 6 of Title 15 CFR (Code of Federal Regulations).

**NIST Interagency Reports (NISTIR)**—A special series of interim or final reports on work performed by NIST for outside sponsors (both government and non-government). In general, initial distribution is handled by the sponsor; public distribution is by the National Technical Information Service, Springfield, VA 22161, in paper copy or microfiche form.

**U.S. Department of Commerce**  
National Institute of Standards and Technology  
325 Broadway  
Boulder, Colorado 80303-3328

**Official Business**  
Penalty for Private Use, \$300